RSC Advances

ROYAL SOCIETY OF CHEMISTRY

www.rsc.org/advances

Graphical Abstract

Py-PCL-*b*-P(NIPAM-*co*-DMAEMA) micelles can present switchable CO_2-temperature dual responses and tunable fluorescence property.

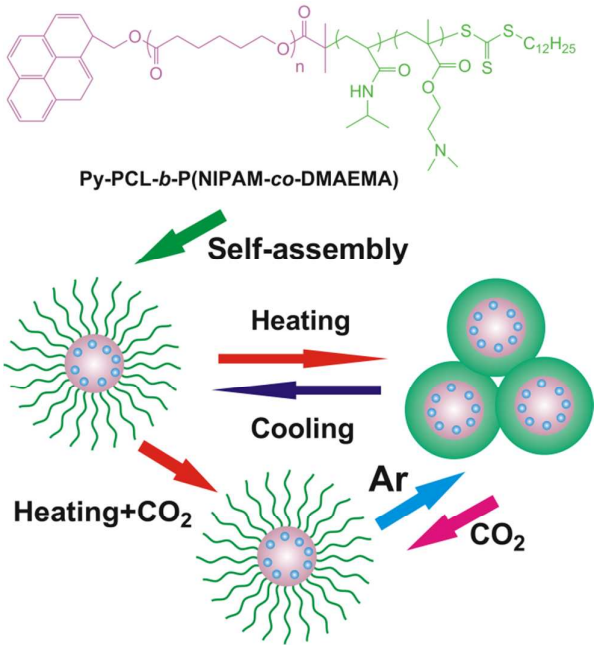

Journal Name

RSCPublishing

ARTICLE

Amphiphilic block copolymer terminated with pyrene group: from switchable CO_2-temperature dual responses to tunable fluorescence

Cite this: DOI: 10.1039/xoxxoooooox

Received ooth January 2012,
Accepted ooth January 2012

DOI: 10.1039/xoxxoooooox

www.rsc.org/

Weizhong Yuan,*[a,b] Jin Shen[a] and Hui Zou[a]

Amphiphilic block copolymer poly(ε-caprolactone)-*block*-poly(N-isopropylacrylamide-*co*-N,N-dimethylaminoethyl methacrylate) terminated with pyrene group (Py-PCL-*b*-P(NIPAM-*co*-DMAEMA)) was synthesized by the combination of ring-opening polymerization (ROP), DCC reaction and reversible addition-fragmentation chain transfer polymerization (RAFT). The micelles self-assembled from the copolymer showed switchable CO_2-temperature dual responses. The copolymerization incorporating DMAEMA was used as a CO_2-responsive trigger into NIPAM, and the lower critical solution temperature (LCST) value could be switched by the gas. The fluorescence intensities and the controlled drug release properties could be adjusted and achieved through altering the temperature of the micelle solution and bubbling CO_2/Ar to the micelle solution.

Recently, considerable interest has been attracted to stimuli-responsive polymers owing to their potential applications in biomedical (e. g. drug and gene delivery) and nano-smart technology (e. g. nano-sensor and nano-reactor) fields.[1-10] Lots of stimuli-responsive polymers have been extensively investigated and reported, such as temperature, pH, light, ionic strength polymers and so on.[11-14] Furthermore, novel type stimuli-responsive polymers, such as carbon dioxide (CO_2)-responsive polymers have attracted great attention due to the availability, nontoxicity, biocompatibility, low cost and abundance of CO_2. CO_2-responsive polymeric materials have been investigated, including polymeric organogels, supramolecular polymers, polymeric vesicles and organic-inorganic hybrid nanomaterils.[15-22] In general, CO_2-responsive polymers are molecules containing amidine functional groups that can react with CO_2 and water to form charged amidinium bicarbonates and be recovered upon CO_2 removal. Taton *et al.* reported the reaction of poly(N-heterocyclic-carbene)s with CO_2 and its use in organocatalysis.[23] Feng *et al.* investigated an amidine-based CO_2-responsive polymer with suitable hydrophobic backbone and amidine pendants derived from polystyrene prepared via a facile route by combination of reversible addition-fragmentation chain transfer polymerization (RAFT) and "click" reaction.[24] Yuan *et al.* prepared an amphiphilic diblock copolymer composed of poly(ethylene oxide) (PEO) and a polyacrylamide bearing an amidine side group and found that its self-assembled vesicle could undergo a reversible expansion and contraction upon exposure to CO_2 and Ar.[25] Incorporating the amidine functional group into a polymer represents a general means to render the polymer CO_2-response, but the synthesis is demanding and the amidine-containing polymers may be hydrolytically unstable.[26] As a result, it is very important to explore more general, robust, and efficient approaches to enable the use of CO_2 as a trigger for a broad range of polymers and materials.[27-30] Zhao *et al.* discovered that poly(N,N-dimethylaminoethyl methacrylate) (PDMAEMA) can react directly with CO_2 in water without functionalization with amidine, which can increase drastically its lower critical solution temperature (LCST), characterizing the transition from a soluble (hydrated) to an insoluble (dehydrated) state.[31] The change in LCST is reversible upon removal of CO_2 using Ar. They also found that the DMAEMA or similar amine-containing monomer units which were incorporated into non-CO_2-responsive, thermoresponse polymer (e. g. poly(N-isopropylacrylamide), PNIPAM) could endow them CO_2-responsive property.[31] Because LCST is a key property for thermo-switchable polymers, it is significant to impart a CO_2-switchable LCST to polymers and make it possible to use CO_2 to trigger reversible structural changes of smart materials. The LCST can be changed and recovered by bubbling CO_2 or Ar. Namely, this kind of polymers can construct the connection of temperature and CO_2 responses. Based on this, the switchable CO_2-temperature dual responsive system deserves further investigation.

Herein, we designed and synthesized an amphiphilic block copolymer poly(ε-caprolactone)-*block*-poly(N-

isopropylacrylamide-*co*-N,N-dimethylaminoethyl methacrylate) terminated with pyrene group (Py-PCL-*b*-P(NIPAM-*co*-DMAEMA)) by the combination of ring-opening polymerization (ROP), DCC reaction and RAFT (Scheme 1). P(NIPAM-*co*-DMAEMA) block is hydrophilic and endowed with thermo-CO_2 dual responses; PCL block is a hydrophobic, good biocompatible and biodegradable segment. The presence of pyrene group provides the fluorescence property for the block copolymer.[32-35] The amphiphilic block copolymer can self-assemble to micelles with CO_2-temperature dual responses. The fluorescence of the micelle solution can be adjusted through the alteration of temperature and bubbling CO_2 or Ar. The controlled drug release of the dual responsive micelles was also investigated.

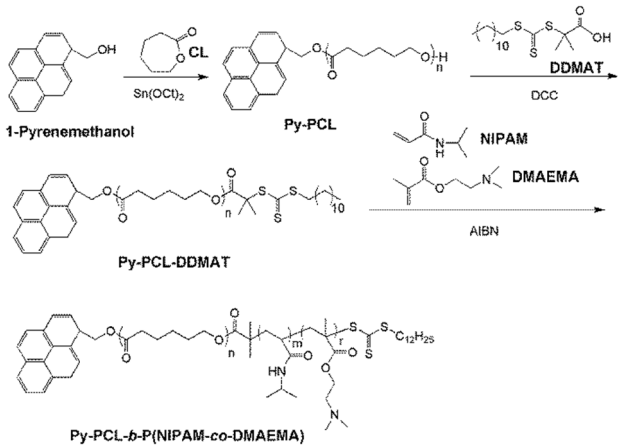

Scheme 1 Synthesis of amphiphilic block copolymer Py-PCL-*b*-P(NIPAM-*co*-DMAEMA).

Experimental

Materials

ε-Caprolactone (CL, Acros Organic, 99%) was purified with CaH2 by vacuum distillation. Tin 2-ethylhexanoate (Sn(Oct)2, Aldrich) was distilled under reduced pressure. 1-Pyrenemethanol, dicyclohexylcarbodiimide (DCC; GL Biochem, Shanghai) and 4-dimethylaminopyridine (DMAP; Fluka, USA) were used as received. S-dodecyl-S'-(α,α'-dimethyl-α''-acetic acid) trithiocarbonate (DDMAT) was prepared according to the literature.[36] 2,2'-Azobisisobutyronitrile (AIBN, Aldrich, 98%) was recrystallized from ethanol. 2-(N,N-Dimethylamino)ethyl methacrylate (DMAEMA) (Acros Organic) was dried over CaH_2 and distilled under reduced pressure. N-isopropyl acrylamide (NIPAM) was purified by recrystallization from a toluene/hexane mixture (1:3).

Characterization

Nuclear magnetic resonance (NMR). ^{1}H NMR spectra of samples were obtained from a Bruker DMX 500 NMR spectrometer with $CDCl_3$ as solvent. The chemical shifts were relative to tetramethylsilane.

Gel permeation chromatography (GPC). The molecular weight and molecular weight distribution were measured on a Waters GPC at 30 ^{o}C. THF was used as eluent and narrow-distributed polystyrene standards were used as calibrations.

Optical transmittances. The optical transmittances of copolymer micelles aqueous solution (30 mg mL^{-1}, deionized water was used as the solvent) at various temperatures were measured at a wavelength of 500 nm on a UV-visible spectrophotometer (Lambda 35, PerkinElmer). The temperature of the sample cell was thermostatically controlled using an external superconstant temperature bath. The solutions were equilibrated for 10 min at each measuring temperature. The LCST values of the copolymer micelles solutions were defined as the temperature producing a 50% decrease in optical transmittance.

Dynamic light scattering spectrophotometer (DLS). The hydrodynamic radius (R_h) of the micelles of copolymer micelles was investigated using DLS techniques. The experiments were performed on a Malven Autosizer 4700 DLS spectrometer. DLS was performed at a scattering angle 90^o. The R_h was obtained by a cumulant analysis.

Transmission electron micrographs (TEM). The morphology of copolymer micelles was observed with a JEOL JEM-2010 TEM at an accelerating voltage of 120 kV. The samples for TEM observation were prepared by placing 10 μL of copolymer micelles solution on copper grids coated with thin films and carbon.

Fluorescence. Fluorescence spectra were performed on a Fluorolog-2 spectrofluorometer (Spex Industries, Edison, NJ) under the control of the dedicated SPEX DM3000F software. The temperature of the micelle solutions was adjusted using water bath and the solutions were equilibrated for 10 min at each temperature. Fluorescence scans were performed in the range of 350-800 nm using increment of 1 nm, and an excitation wavelength of 340 nm, which is at the maximum absorption peak for pyrene. The concentrations of the micelles are 2.3 mg mL^{-1}.

Synthesis of Py-PCL

Py-PCL was synthesized by ROP of CL with 1-pyrenemethanol as the initiator. The detailed procedure was described as follows. CL (10.00 g, 87.6 mmol), 1-pyrenemethanol (0.50 g, 2.2 mmol of hydroxyl groups), $Sn(Oct)_2$ catalyst (87.7 μmmol) and a magnetic stirrer were added into a flame-dried polymerization tube. The tube then connected to a Schlenkline, where an exhausting-refilling process was repeated three times. The polymerization tube was sealed in argon atmosphere. Under stirring, the bulk polymerization was carried out at 115 ^{o}C for 24 h. The crude polymer was dissolved in methylene chloride and precipitated in methanol for three times. The purified Py-PCL was dried in a vacuum until constant weight (Yield: 91%). $M_{n,NMR}$=4792 g/mol, $M_{n,GPC}$=4170 g/mol, M_w/M_n=1.27. ^{1}H NMR ($CDCl_3$, δ, ppm): 8.00-8.30 (protons in pyrene group), 5.84 (pyrene-CH_2O), 4.06 (OOCCH$_2$CH$_2$CH$_2$CH$_2$CH_2O), 3.64 (OOCCH$_2$CH$_2$CH$_2$CH$_2$CH_2OH), 2.30 (OOCCH_2CH$_2$CH$_2$CH$_2$CH$_2$O), 1.65

(OOCCH$_2$C*H*$_2$CH$_2$C*H*$_2$CH$_2$O), 1.39 (OOCCH$_2$CH$_2$C*H*$_2$CH$_2$CH$_2$O).

Synthesis of Py-PCL-DDMAT

Py-PCL (7.0 g, 1.46 mmol), DDMAT (5.1 g, 14.1 mmol), DCC (2.9 g, 14.1 mmol) and DMAP (0.94 g, 7.69 mmol) were dissolved in 40 mL of anhydrous dichloromethane, and the reaction was performed at room temperature for 48 h under argon atmosphere. The reaction byproduct dicyclohexylcarbodiurea was removed by filtration. The purified product was obtained after removing of solvent and precipitating in methanol (Yield: 70%).

$M_{n,NMR}$=5150 g/mol, $M_{n,GPC}$=4450 g/mol, M_w/M_n=1.29. ^{1}H NMR ($CDCl_3$, δ, ppm): 8.00-8.30 (protons in pyrene group), 5.86 (pyrene-C*H*$_2$O), 4.06 (OOCCH$_2$CH$_2$CH$_2$CH$_2$C*H*$_2$O), 3.50 (OOCCH$_2$CH$_2$CH$_2$CH$_2$C*H*$_2$OOCC(CH$_3$)$_2$), 3.26 (SC*H*$_2$(CH$_2$)$_{10}$CH$_3$), 2.32 (OOCC*H*$_2$CH$_2$CH$_2$CH$_2$CH$_2$O), 1.65 (OOCCH$_2$C*H*$_2$CH$_2$C*H*$_2$CH$_2$O, (C*H*$_3$)$_2$CS), 1.40 (OOCCH$_2$CH$_2$C*H*$_2$CH$_2$CH$_2$O, SCH$_2$(C*H*$_2$)$_{10}$CH$_3$), 0.88 (SCH$_2$(CH$_2$)$_{10}$C*H*$_3$).

Synthesis of Py-PCL-*b*-P(NIPAM-*co*-DMAEMA)

Py-PCL-*b*-P(NIPAM-*co*-DMAEMA) was synthesized by RAFT with Py-PCL-DDMAT as the macro-RAFT agent. NIPAM (2.716 g, 24 mmol), DMAEMA (0.164 g, 1 mmol) and Py-PCL-DDMA (1.0 g, 0.194 mmol) were dissolved in 6 mL of dioxane, and then AIBN (8.2 mg, 49 μmol) was added. The flask was degassed with three freeze-evacuate-thaw cycles. The polymerization reaction was performed at 70 ^{o}C for 7 h. Py-PCL-*b*-P(NIPAM-*co*-DMAEMA) copolymer was obtained after precipitation in diethyl ether twice (Yield: 82%).

$M_{n,NMR}$=16658 g/mol, $M_{n,GPC}$=11320 g/mol, M_w/M_n=1.26. ^{1}H NMR ($CDCl_3$, δ, ppm): 8.00-8.30 (protons in pyrene group), 5.92-6.87 (CON*H*), 4.07 (OOCCH$_2$CH$_2$CH$_2$CH$_2$C*H*$_2$O, NHC*H*, COOC*H*$_2$CH$_2$N), 2.59 (COOCH$_2$C*H*$_2$N), 2.31 (OOCC*H*$_2$CH$_2$CH$_2$CH$_2$CH$_2$O, N(C*H*$_3$)$_2$), 2.13 (CH$_2$C*H*(CO)), 1.66 (OOCCH$_2$C*H*$_2$CH$_2$C*H*$_2$CH$_2$O, C*H*$_2$CH(CO), C*H*$_2$C(CH$_3$)), 1.40 (OOCCH$_2$CH$_2$C*H*$_2$CH$_2$CH$_2$O), 1.16 (NHCH(C*H*$_3$)$_2$, CH$_2$C(C*H*$_3$)).

Preparation of Py-PCL-*b*-P(NIPAM-*co*-DMAEMA) micelles and doxorubicin (DOX)-loaded micelles

Py-PCL-*b*-P(NIPAM-*co*-DMAEMA) micelles were prepared by self-assembly of the block copolymer in water. The block copolymer (50 mg) was dissolved into DMF (10 mL). Then the solution was dialyzed against deionized water with a dialysis tube (molecular weight cut-off: 3500 Da) for 3 days at 25 ^{o}C.

The anti-cancer drug of DOX was chosen to be used as the model drug. The mixture of doxorubicin hydrochloride (DOX•HCl) (15 mg), Et_3N (3 mL) and DMF (10 mL) was stirred at room temperature overnight and then DOX/DMF solution was obtained. 50 mg of Py-PCL-*b*-P(NIPAM-*co*-DMAEMA) copolymer was added. After stirring for 3 h, the mixture was dialyzed against phosphate buffer saline (PBS) solution with a dialysis tube (molecular weight cut-off: 3500 Da) at 25 ^{o}C for 24 h and replaced with fresh PBS solution at the interval of 6 h.

Results and discussion

Synthesis of Py-PCL-*b*-P(NIPAM-*co*-DMAEMA) amphiphilic block copolymer

Py-PCL-*b*-P(NIPAM-*co*-DMAEMA) amphiphilic block copolymer was synthesized by three steps. Firstly, Py-PCL was synthesized by ROP of CL with 1-pyrenemethanol as the initiator. Sn(Oct)$_2$ was used as the catalyst. The structure of Py-PCL was characterized by ^{1}H NMR spectrum (Fig. 1(a)). Besides the proton signals of the PCL chain and pyrene group, the signal at 3.64 ppm assigned to the methylene protons next to the terminal hydroxyl groups can be detected. The average-number molecular weight ($M_{n,NMR}$) of Py-PCL was calculated by equation (1).

$$M_{n,NMR}\,(\text{Py-PCL})=(I_e/I_{e'}+1)\times 114.14+232.29 \quad (1)$$

Here, 114.14 is the value of molecular weight of CL monomer and 232.29 is the value of molecular weight of 1-pyrenemethanol. The $M_{n,NMR}$ of Py-PCL was 4792 g/mol. According to GPC trace (Fig. 2), the average-number molecular weight of Py-PCL was 4170 g/mol.

Secondly, Py-PCL-DDMAT macroinitiator was prepared by DCC reaction of terminal hydroxyl group of Py-PCL with carboxyl group of DDMAT. The amount of DDMAT was excess to ensure the complete transformation of hydroxyl group of Py-PCL. Fig. 1(b) shows the ^{1}H NMR spectrum of Py-PCL-DDMAT. The $M_{n,NMR}$ and $M_{n,GPC}$ of Py-PCL-DDMAT were 5150 g/mol and 4450 g/mol, respectively.

Finally, Py-PCL-*b*-P(NIPAM-*co*-DMAEMA) amphiphilic block copolymer was synthesized by RAFT of NIPAM and DMAEMA with Py-PCL-DDMAT as the macroinitiator. The feed ratio of NIPAM to DMAEMA was 96:4 (mol%:mol%). As shown in ^{1}H NMR spectrum (Fig. 1(c), all the protons in Py-PCL-*b*-P(NIPAM-*co*-DMAEMA) can be found. The $M_{n,NMR}$ and $M_{n,GPC}$ of Py-PCL-*b*-P(NIPAM-*co*-DMAEMA) were 16658 g/mol and 11320 g/mol, respectively. The fact that $M_{n,GPC}$ was lower than $M_{n,NMR}$ should be attributed to the possible absorption of P(NIPAM-*co*-DMAEMA) onto the GPC column which resulted in an increase of retention time and led to lower molecular weight detected by GPC.

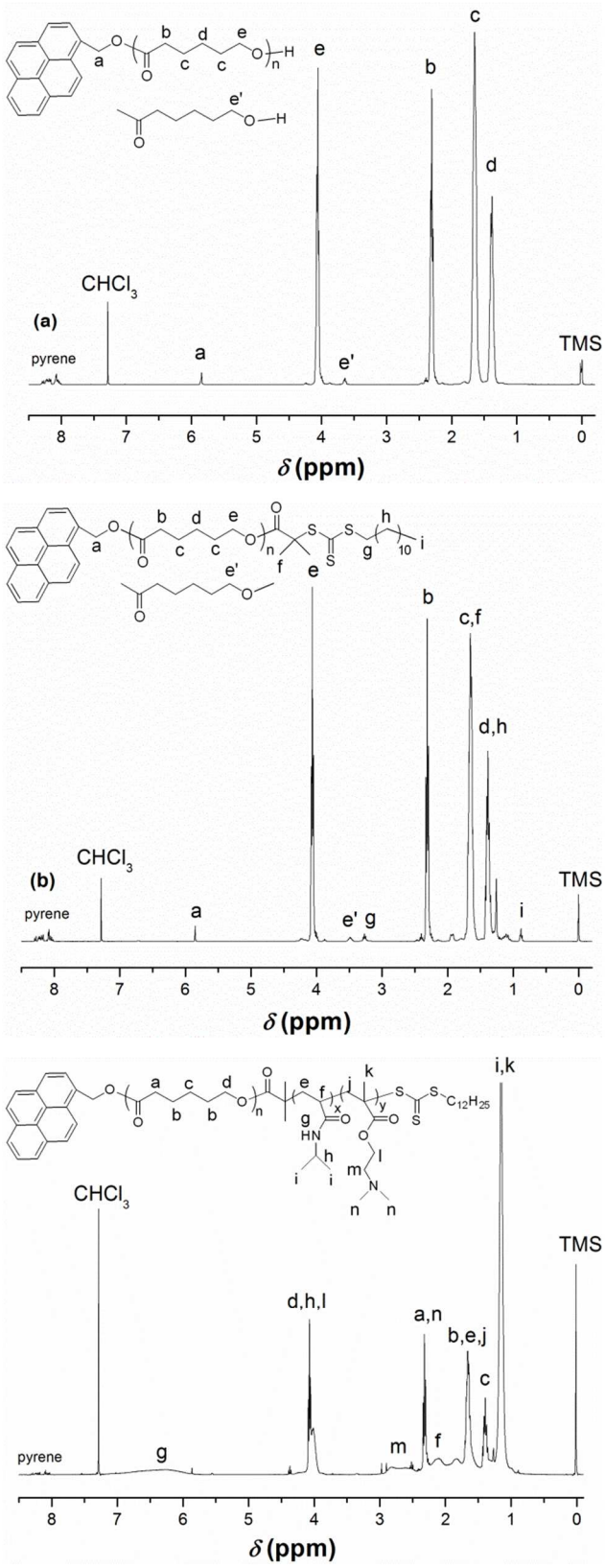

Fig. 1 ^{1}H NMR spectra of (a) Py-PCL, (b) Py-PCL-DDMAT and (c) Py-PCL-*b*-P(NIPAM-*co*-DMAEMA).

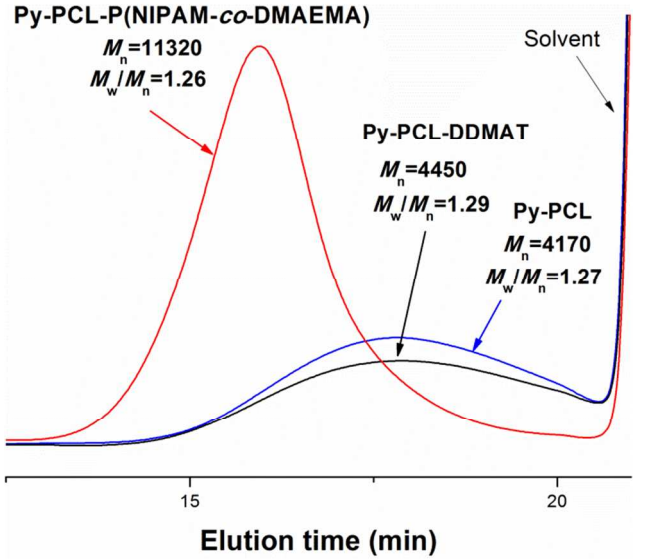

Fig. 2 GPC traces of Py-PCL, Py-PCL-DDMAT and Py-PCL-*b*-P(NIPAM-*co*-DMAEMA).

Self-assembly and thermo-CO_2 dual responses of Py-PCL-*b*-P(NIPAM-*co*-DMAEMA) amphiphilic block copolymer

As an amphiphilic copolymer, Py-PCL-*b*-P(NIPAM-*co*-DMAEMA) can self-assemble into micelles in aqueous solution with hydrophilic P(NIPAM-*co*-DMAEMA) shell and hydrophobic Py-PCL core. The morphologies of the copolymer micelles at 25 °C, 42 °C and after passing CO_2 (5 min), after passing Ar (5 min) were shown in Fig. 3. At 25 °C, the spherical micelles can be self-assembled from Py-PCL-*b*-P(NIPAM-*co*-DMAEMA) in water (Fig. 3(a)). When the temperature increased to 42 °C, the micelles tended to aggregate into aggregates due to the hydrophilic-hydrophobic transition of P(NIPAM-*co*-DMAEMA) shell (Fig. 3(b)). After bubbling CO_2 for 5 min, the aggregation of micelles reduced because the P(NIPAM-*co*-DMAEMA) segment became hydrophilic due to the reaction of DMAEMA units with CO_2 and water and the formation of bicarbonate salts of protonated amine groups. Therefore, the micelle aggregation was relieved, as shown in Fig. 3(c). But the serious aggregation of micelles occurred again after bubbling Ar to the micelle solution (Fig. 3(d)), which should attributed to the formation of deprotonated amine groups. The micelle morphology can be reversibly adjusted through the alteration of temperature and bubbling CO_2/Ar.

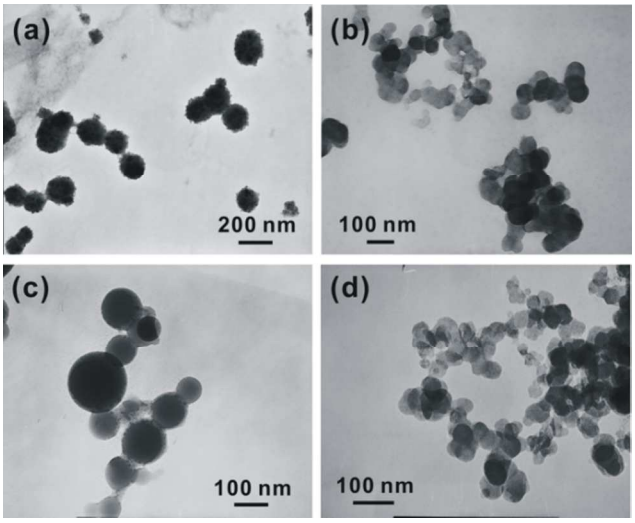

Fig. 3 TEM images of Py-PCL-*b*-P(NIPAM-*co*-DMAEMA) micelles at (a) 25 °C, (b) 42 °C and (c) after passing CO_2 (5 min), (d) after passing Ar (5 min).

Fig. 4(a) shows the transmittance curves of Py-PCL-*b*-P(NIPAM-*co*-DMAEMA) micelle solutions. It can be seen that the transmittance curve shows sharp transition during heating process for the initial solution. The LCST value of the copolymer was 36.0 °C. But after bubbling CO_2 to the solution for 5 min, the transmittance increased above 60% and no obvious transition occurred during the heating process. After bubbling Ar for 5 min, the sharp transition during heating process appeared again and the LCST value was 37.1 °C. The insert photograph shows the reversible transparency-turbidity transition of copolymer micelle solutions after heating-cooling and CO_2/Ar cycles. The expanded inset images could be found in Fig. S1 (ESI). The reversible transmittance curves of Py-PCL-*b*-P(NIPAM-*co*-DMAEMA) micelle solutions at 25 °C and 50 °C respectively could be found in Fig. S2 (ESI).

Fig. 4(b) shows the plot of the hydrodynamic radius (R_h) of Py-PCL-*b*-P(NIPAM-*co*-DMAEMA) micelles in water as a function of temperature. In the lower temperature ranges, the R_h values were relatively small and changed slightly. However, the values increased in the higher temperature ranges. At low temperatures, the P(NIPAM-*co*-DMAEMA) chains in micelles existed in random coil conformation owing to the hydrogen-bonding interaction between the polymers and water molecules. When the temperature increased to a critical value, the polymer chains shrank into a globular structure because the hydrogen bonds between the polymers and water collapsed and became hydrophobic. Therefore, the micelles tended to aggregate into aggregates with large size. After bubbling CO_2 for 5 min, the the R_h values were relatively small and changed slightly with the increase of temperature because the protonated amine groups made the P(NIPAM-*co*-DMAEMA) chains remain hydrophilic at high temperature. As a result, the aggregation did not occur at high temperature range. If Ar was bubbled into the solution, CO_2 would be expelled from the solutions by Ar and amine groups were deprotonated at high temperature. Therefore, the hydrophobic P(NIPAM-*co*-DMAEMA) chains at high temperature collapsed and the micelles aggregated to form aggregates. Due to the presence of partial protonated amine groups, the aggregation of micelles was weaker than that of initial solution.

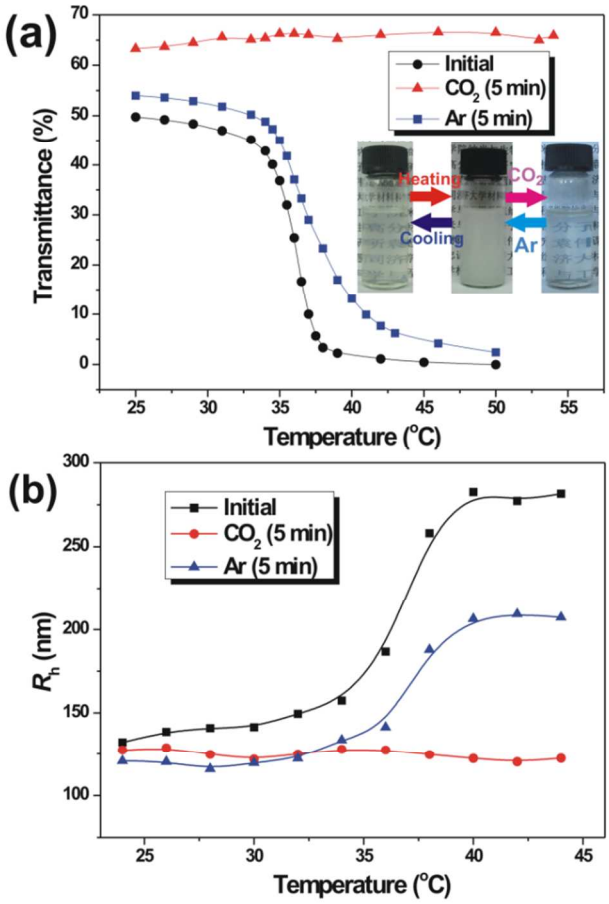

Fig. 4 (a) Transmittance curves of Py-PCL-*b*-P(NIPAM-*co*-DMAEMA) micelle solutions at different conditions. The insert photograph: the reversible transparency-turbidity transition of copolymer micelle solution after heating-cooling cycle and bubbling CO_2-Ar cycle. (Concentration: 2.3 mg/mL) and (b) Temperature dependence of hydrodynamic radius (R_h) for Py-PCL-*b*-P(NIPAM-*co*-DMAEMA) micelles at different conditions. (Concentration: 2.3 mg/mL)

The schematic self-assembly process of Py-PCL-*b*-P(NIPAM-*co*-DMAEMA) and the CO_2-temperature dual responses was shown in Fig. 5. The reversible hydrophilic-hydrophobic change of P(NIPAM-*co*-DMAEMA) chains during the heating-cooling processes led to the reversible aggregation/disaggregation behaviours. After bubbling CO_2, the micelles still remained stable at high temperature. But bubbling Ar to the solution would lead to the aggregation of micelles due to the hydrophilicity-hydrophobicity transition of P(NIPAM-*co*-DMAEMA) chains after bubbling CO_2/Ar at high temperature.

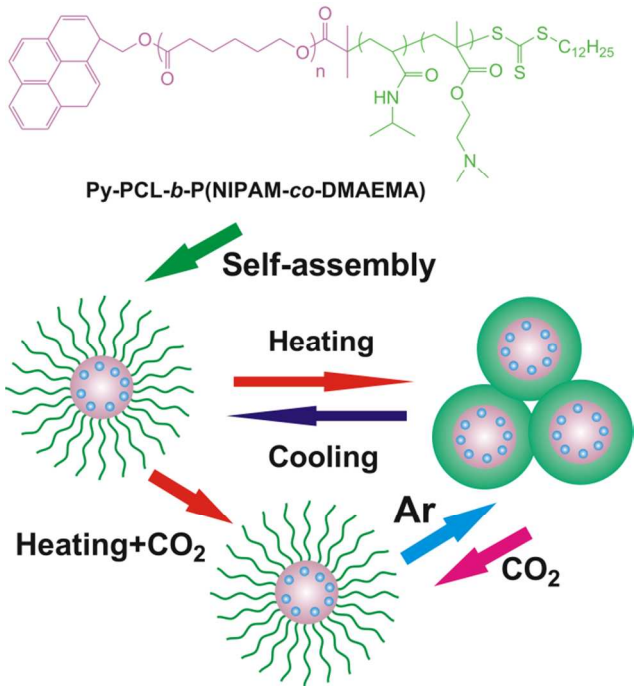

Fig. 5 The schematic self-assembly process of Py-PCL-*b*-P(NIPAM-*co*-DMAEMA) and the CO_2-temperature dual responses.

In order to confirm the temperature and CO_2 responses of Py-PCL-*b*-P(NIPAM-*co*-DMAEMA), the ^1H NMR spectra of the polymer in D_2O at different temperature and passing CO_2 or Ar were recorded, as shown in Fig. 6. Compared to the proton peaks in N-isopropylacrylamide and dimethylaminoethyl at 25 ^oC, the intensities of peaks of protons decreased at 45 ^oC. At high temperature range, the hydrophilicity of P(NIPAM-*co*-DMAEMA) was obviously weakened. After bubbling CO_2 to the solution for 5 min, the intensities of proton peaks in N-isopropylacrylamide and dimethylaminoethyl increased to some degree. Because of the reaction of DMAEMA units with CO_2 and water and the formation of bicarbonate salts of protonated amine groups, the P(NIPAM-*co*-DMAEMA) chains can maintain the hydrophilic state. However, after bubbling Ar to the solution for 5 min, CO_2 was removed and replaced by Ar. As a result, the protonated amine groups were deprotonated. At high temperature (42 ^oC), the P(NIPAM-*co*-DMAEMA) chains changed from hydrophilic to hydrophobic. The intensities of the proton peaks of P(NIPAM-*co*-DMAEMA) obviously decreased.

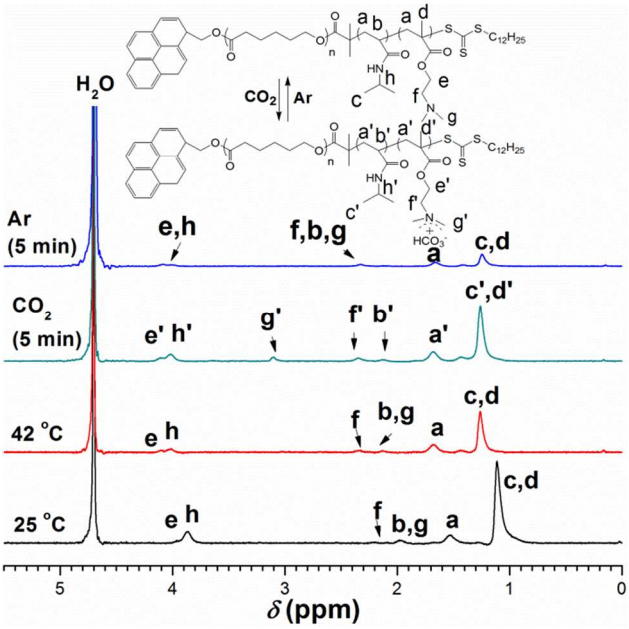

Fig. 6 ^1H NMR spectra of Py-PCL-*b*-P(NIPAM-*co*-DMAEMA) in D_2O conducted at 25 ^oC, 42 ^oC and before and after passing CO_2 (5 min) or Ar (5 min) through the solution (42 ^oC).

Tunable fluorescence of Py-PCL-*b*-P(NIPAM-*co*-DMAEMA) micelle solution

Due to the fluorescence of the pyrene groups, the Py-PCL-*b*-P(NIPAM-*co*-DMAEMA) micelles would also present fluorescent properties. Moreover, in the micelles, the pyrene groups were at the core part and the fluorescence intensity is influenced by the spatial conformation variation of the P(NIPAM-*co*-DMAEMA), which could be adjusted by the alteration of temperature or bubbling CO_2/Ar.

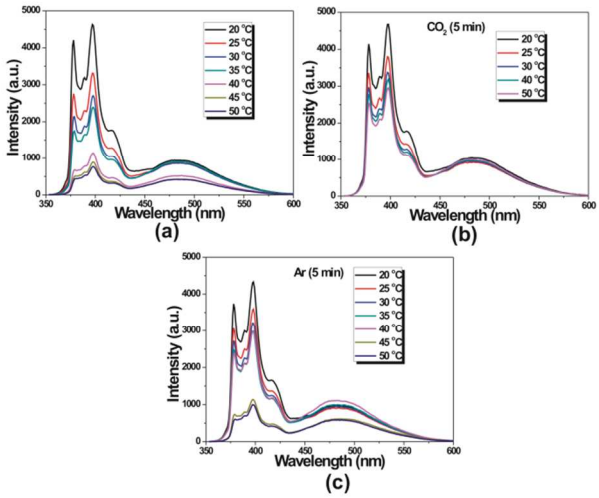

Fig. 7 The fluorescence spectra of Py-PCL-*b*-P(NIPAM-*co*-DMAEMA) micelle solutions (a) with different temperature, (b) with different temperature after bubbling CO_2 for 5 min and (c) with different temperature after bubbling Ar for 5 min.

As shown in Fig. 7(a), the fluorescence intensity of Py-PCL-*b*-P(NIPAM-*co*-DMAEMA) micelle solution decreased with the increase of the temperature, especially when the temperature was higher than the LCST value of the solution. The main reason is that when the temperature changed, the conformation of P(NIPAM-*co*-DMAEMA) in aqueous solutions would change, resulting in the change of the light transmittance of the system. After CO_2 was bubbled into the solution, the decrease of fluorescence intensity of the micelle solution was much less than that of the solution without bubbling CO_2 in the temperature range above the LCST value, as shown in Fig. 7(b). After bubbling CO_2, the P(NIPAM-*co*-DMAEMA) chains still remained hydrophilic at high temperature. As shown in Fig. 8(c), when Ar was bubbled into the solution for 5 min, CO_2 was removed and the P(NIPAM-*co*-DMAEMA) chains were changed to hydrophobicity. At high temperature ranges, the fluorescence intensity of the micelle solution rapidly decreased. Therefore, the tunable fluorescence properties of the Py-PCL-*b*-P(NIPAM-*co*-DMAEMA) micelle solution could be achieved through altering the temperature of the solution or bubbling CO_2/Ar to the micelle solution.

Controlled drug-release of Py-PCL-*b*-P(NIPAM-*co*-DMAEMA) micelle

The controlled drug-release behaviours of the Py-PCL-*b*-P(NIPAM-*co*-DMAEMA) micelles at 25 °C, 40 °C and 40 °C (with alternative CO_2/Ar) were investigated. Model drug (DOX) loading content (DLC) and drug loading efficiency (DLE) were calculated according to the following formulae:

DLC (wt%)=(weight of loading DOX/weight of polymer)×100%

DLE (wt%)=(weight of loading DOX/weight of DOX in feed)×100%

The final DLC and DLE of supramolecular block copolymer micelles were 6.1% and 21.7%, respectively.

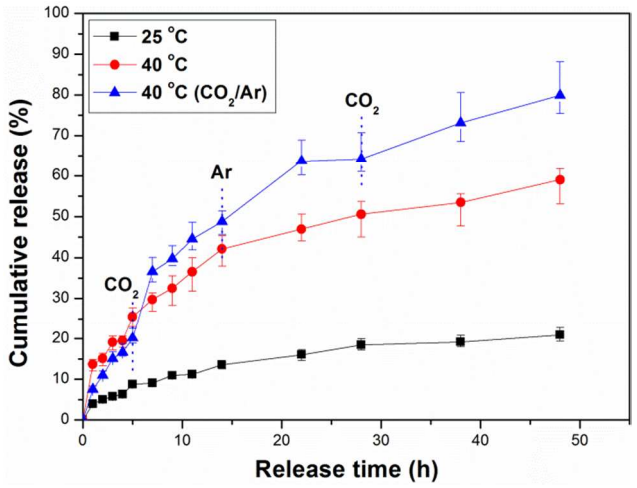

Fig. 8 Controlled release of DOX at 25 °C, 40 °C and 40 °C with alternatively bubbling CO_2/Ar.

As shown in Fig. 8, the drug release profile from micelles shows greater changes with the temperature alternations around the LCST of copolymer. Under the LCST (25 °C), the highly hydrated P(NIPAM-*co*-DMAEMA) segments stabilized the hydrophobic-hydrophilic core-shell structure of micelles, and only small amount of drug could diffuse out from the micelles. As a result, the drug release was slow and about 79% drug still remained in the core of the micelles after 48 h. But, when the temperature was raised above the LCST (40 °C), the drug release was accelerated due to the temperature-induced structural changes of the micelles. Namely, the P(NIPAM-*co*-DMAEMA) shell became hydrophobic, and the micellar core-shell structure was deformed. Therefore, the hydrophobic DOX incorporated in core diffused out quickly and about 59% drug was released from the micelles after 48 h. Obviously, the release rate of model drug DOX from the micelles could be effectively controlled by changing the solution temperatures. Moreover, the release curve of DOX with alternative CO_2/Ar bubbling presented a fast-slow alternation feature, which should be attributed to the extension-retraction motion of the micelles under the alternative stimulation of CO_2/Ar. As a result, about 80% DOX was released from the micelles after 48 h.

Conclusions

The novel amphiphilic copolymer with terminal pyrene group (Py-PCL-*b*-P(NIPAM-*co*-DMAEMA)) was synthesized successfully by the combination of ROP, DCC reaction and RAFT. The copolymer could self-assemble to micelles with Py-PCL core and P(NIPAM-*co*-DMAEMA) shell. The micelles show switchable CO_2-temperature dual responses. Without bubbling CO_2, the copolymer presented a LCST value (36 °C) and revealed thermo-response. After bubbling CO_2, the P(NIPAM-*co*-DMAEMA) chains remained hydrophilic at high temperature. Removing CO_2 by Ar would lead to the appearance of the similar LCST value (37.1 °C). Investigation shows that the copolymer micelle solution could present fluorescence and the fluorescence intensities could be adjusted through altering the temperature of solution or bubbling CO_2/Ar to the solution. Moreover, as a drug delivery system, the DOX-loaded micelles accomplished the controlled release of DOX by changing the temperature and alternatively bubbling CO_2/Ar to the solution.

Acknowledgements

The authors thank the financial supports the National Key Technology R&D Program (no. 2012BAI15B061), the National Basic Research Program of China (973 Program: 2011CB013805) and the National High Technology Research and Development Program (no. 2013AA032202).

Notes and references

[a]Institute of Nano and Bio-polymeric Materials, School of Materials Science and Engineering, Tongji University, 4800 Cao'an Road, Shanghai 201804, People's Republic of China. Fax: +86 21 69584723; Tel: +86 21 69580234; E-mail: yuanwz@tongji.edu.cn

[b]Key Laboratory of Advanced Civil Materials, Ministry of Education, 4800 Cao'an Road, Shanghai 201804, People's Republic of China. Fax: +86 21 69584723; Tel: +86 21 69580234; E-mail: yuanwz@tongji.edu.cn

1 P. Schattling, F. D. Jochum and P. Theato, *Polym. Chem.*, 2014, **5**, 25-36.
2 F. D. Jochum and P. Theato, *Chem. Soc. Rev.*, 2013, **42**, 7468-7483.
3 M. Huo, J. Y. Yuan, L. Tao and Y. Wei, *Polym. Chem.*, 2014, **5**, 1519-1528.
4 Q. L. Zhang, N. Vanparijs, B. Louage, B. G. De Geest and R. Hoogenboom, *Polym. Chem.*, 2014, **5**, 1140-1144.
5 W. Z. Yuan, H. Zou, W. Guo, T. X. Shen and J. Ren, *Polym. Chem.*, 2013, **4**, 2658-2661.
6 W. Z. Yuan, W. Guo, H. Zou and J. Ren, *Polym. Chem.*, 2013, **4**, 3934-3937.
7 W. Z. Yuan, T. X. Shen, J. J. Wang and H. Zou, *Polym. Chem.*, 2014, **5**, 3968-3971.
8 W. Z. Yuan and W. Guo, *Polym. Chem.*, 2014, **5**, 4259-4267.
9 W. Z. Yuan, H. Zou, W. Guo, A. Wang and J. Ren, *J. Mater. Chem.*, 2012, **22**, 24783-24791.
10 W. Z. Yuan and J. J. Wang, *RSC Adv.*, 2014, **4**, 38855-38858.
11 K. L. Hamner, C. M. Alexander, K. Coopersmith, D. Reishofer, C. Provenza and M. M. Maye, *ACS Nano*, 2013, **7**, 7011-7020.
12 A. J. Convertine, C. Diab, M. Prieve, A. Paschal, A. S. Hoffman, P. H. Johnson and P. S. Stayton, *Biomacromolecules*, 2010, **11**, 2904-2911.
13 Y. Zhao, *Macromolecules*, 2012, **45**, 3647-3657.
14 S. V. Solomatin, T. K. Bronich, T. W. Bargar, A. Eisenberg, V. A. Kabanov and A. V. Kabanov, *Langmuir*, 2003, **19**, 8069-8076.
15 C. Liang, Q. X. Liu and Zhenghe Xu, *ACS Appl. Mater. Interfaces*, 2014, **6**, 6898-6904.
16 B. W. Liu, H. Zhou, S. T. Zhou, H. J. Zhang, A. C. Feng, C. M. Jian, J. Hu, W. P. Gao and J. Y. Yuan, *Macromolecules*, 2014, **47**, 2938-2946.
17 Y. Ding, S. L. Chen, H. P. Xu, Z. Q. Wang, X. Zhang, T. H. Ngo and M. Smet, *Langmuir*, 2010, **26**, 16667-16671.
18 Q. Yan and Y. Zhao, *Chem. Commun.*, 2014, **50**, 11631-11641.
19 N. Li, L. Thia and X. Wang, *Chem. Commun.*, 2014, **50**, 4003-4006.
20 L. Q. Xu, B. Zhang, M. Sun, L. Hong, K. G. Neoh, E. T. Kang and G. D. Fu, *J. Mater. Chem. A*, 2013, **1**, 1207-1212.
21 S. S. Satav, S. Bhat and S. Thayumanavan, *Biomacromolecules* 2010, **11**, 1735-1740.
22 H. B. Liu, Y. Zhao, C. A. Dreiss and Y. J. Feng, *Soft Matter*, 2014, **10**, 6387-6391.
23 J. Pinaud, J. Vignolle, Y. Gnanou and D. Taton, *Macromolecules*, 2011, **44**, 1900-1908.
24 Z. R. Guo, Y. J. Feng, Y. Wang, J. Y. Wang, Y. F. Wu and Y. M. Zhang, *Chem. Commun.*, 2011, **47**, 9348-9350.
25 Q. Yan, R. Zhou, C. K. Fu, H. J. Zhang, Y. W. Yin and J. Y. Yuan, *Angew. Chem. Int. Ed.*, 2011, **50**, 4923-4927.
26 P. G. Jessop, L. Kozycz, Z. G. Rahami, D. Schoenmakers, A. R. Boyd, D. Wechsler, A. M. Holland, *Green Chem.*, 2011, **13**, 619-623.
27 D. Nagai, A. Suzuki, Y. Maki and H. Takeno, *Chem. Commun.*, 2011, **47**, 8856-8858.
28 S. Kumar, X. Tong, Y. L. Dory, M. Lepage and Y. Zhao, *Chem. Commun.*, 2013, **49**, 90-92.
29 N. Che, S. Yang, H. L. Kang, R. G. Liu, Z. Li, Z. J. Liu, P. P. Li, X. Z. Qu and Y. Huang, *Polym. Chem.*, 2014, DOI: 10.1039/C4PY00987H
30 Q. Yan and Y. Zhao, *J. Am. Chem. Soc.*, 2013, **135**, 16300-16303
31 D. H. Han, X. Tong, O. Boissière and Yue Zhao, *ACS Macro Lett.*, 2012, **1**, 57-61.
32 E. Biver, M. Berta, A. D'Aléo, T. Phan, S. Maria, F. Fages, D. Gigmes, M. Sentis and P. Delaporte, *ACS Appl. Mater. Interfaces*, 2014, **6**, 41-48.
33 T. M. Figueira-Duarte and K. Müllen, *Chem. Rev.*, 2011, **111**, 7260-7314.
34 W. Z. Yuan, X. F. Li, S. Y. Gu, A. M. Cao, J. Ren, *Polymer*, 2011, **52**, 658-666.
35 H. Zou, W. Guo and W. Z. Yuan, *J. Mater. Chem. B*, 2013, **1**, 6235-6244.
36 J. T. Lai, D. Filla and R. Shea, *Macromolecules,* 2002, **35**, 6754-6756.

